



# Graphene-Based Hyperbolic Metamaterial Acting as Tunable THz Power Limiter

Bartosz Janaszek , Anna Tyszka-Zawadzka , and Paweł Szczepański

**Abstract**—In this paper, we investigate the possibility of employing a graphene-based hyperbolic metamaterial as a tunable optical power limiter and/or controllable laser noise suppressor for terahertz frequency range. This is the first time that the mentioned functionalities are obtained with a voltage-controlled nonlinear hyperbolic metamaterial utilizing graphene. We believe that such structures, feasible by means of planar deposition techniques, will find practical applications in THz systems requiring optical power limiting.

**Index Terms**—Graphene, hyperbolic metamaterials, nanostructures, optical properties, terahertz.

## I. INTRODUCTION

TERAHERTZ (THz) radiation is of outstanding interest in both technology and science, offering unique applications in a wide range of fields, such as imaging [1], [2], biosensing [3], filtering [4], absorbing [5], information and communications technology (ICT) [6], as well as electromagnetic waveguiding [7], [8]. To expand the applications of terahertz radiation, new materials and device designs are required. These will open up new opportunities in further development of compact THz components/systems for more efficient operation, detection, modulation, and radiation generation. The development of intense THz sources and their applications demands optical power limiters (OPLs), i.e., optical components, that protect their sensitive components, such as photodetectors and cameras, from damaged caused by high-power radiation.

Since the first introduction of a parametric subharmonic oscillator working as an OPL in 1962 [9] by Siegman, various materials, mechanisms, structures and devices have been considered in this context, including semiconductors, photonic crystals or structures supporting topological edge states [10], [11], [12], [13], [14], [15], [16], [17], [18]. However, conventional OPL solutions often reveal substantial shortcomings, such as a narrow band of spectral operation, polarization sensitivity, and relatively small transmission in on-state, which significantly limits their practical applicability.

Manuscript received 30 November 2022; revised 20 January 2023, 15 April 2023, and 26 April 2023; accepted 26 April 2023. Date of publication 1 May 2023; date of current version 15 May 2023. (Corresponding author: Bartosz Janaszek)

Bartosz Janaszek and Anna Tyszka-Zawadzka are with the Warsaw University of Technology, 00-661 Warsaw, Poland (e-mail: bartosz.janaszek@pw.edu.pl; anna.zawadzka1@pw.edu.pl).

Paweł Szczepański is with the Warsaw University of Technology and National Institute of Telecommunications, 00-661 Warsaw, Poland (e-mail: pawel.szczepanski@pw.edu.pl).

Color versions of one or more figures in this article are available at <https://doi.org/10.1109/JSTQE.2023.3271766>.

Digital Object Identifier 10.1109/JSTQE.2023.3271766

More recently, to address the drawback of conventional THz photonic devices, optical metamaterial platform has been employed [19], [20], [21], [22], [23], [24], [25], [26], [27], [28], [29], [30], [31]. Due to their tailorable electromagnetic response, optical metamaterials have been perceived as natural candidates for many practical THz components such as modulators [19], [20], [21], [22], polarizers [23], absorbers [24], [25], switches [26], waveguides [27], [28]. In particular, hyperbolic metamaterials (HMMs), a special class of metamaterials characterized with extreme anisotropy resulting in an unusual hyperbolic dispersion, have been considered in many THz applications, such as tunable spatial filtering [32], ultrabroad bandpass filtering [33], controllable phase and amplitude modulation [34], [35] as well as omnidirectional absorption [36]. Among them, HMMs incorporating graphene, i.e., a two-dimensional lattice of carbon atoms supporting highly tunable and low loss plasmon propagation in the THz range [37], have been recognized for their usability in constructing absorbers [5], [38], [39], diffractionless lenses [40] and antennas [41]. Additionally, it has been reported that non-linear properties of graphene may be employed to achieve enhanced third harmonic generation [42], [43] or coherent generation of THz frequencies [44].

Until now, a great majority of studies concerning optical metamaterials were focused on achieving optical switching [45], [46], [47], [48], [49], [50], [51]. Only a limited number of publications in the field of optical metamaterials has covered the subject of optical power limiting. So far, intensity-dependent polarization rotation, which may be employed to obtain OPL, has been demonstrated in a varactor-based chiral metadvice [52]. Moreover, microwave metamaterials based on varactor diodes have been proven to reveal narrowband power-dependent transmission for frequencies near resonance [53], [54]. For achieving enhanced optical power limiting a planar negative-index metamaterial concept have been proposed [55]. At THz frequencies semiconducting plasmonic metamaterials have been successfully demonstrated to reveal saturable absorption, that may be applied to achieve OPL functionality [56]. However, due to employed physical mechanism, the presented structure revealed relatively narrowband operation and high insertion loss (up to 70% of light is transmitted in the on-state) [56].

In our work, we investigate planar hyperbolic metamaterial with graphene as a plasmonic material as a mean to achieve a tunable optical power limiter operating within THz spectral range, that is able to cut off the transmission by reflecting radiation when optical power reaches and exceeds a certain threshold level. Within our analysis, we consider a

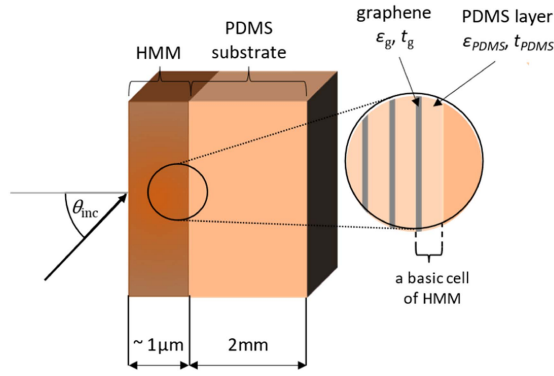


Fig. 1. Schematic of the proposed optical system (not in scale).

subwavelength lithography-free multilayer planar stack, which can be fabricated by means of well-established deposition techniques and reveal broader spectral range of operation than resonator-based solution [57], while maintaining high transmission in the on-state and complete rejection in the off-state. Such optical power limiter can be employed to protect sensitive optoelectronic components/systems, such as photodiodes, sensors, from damage caused by e.g., high power laser radiation. Moreover, by changing the biasing potential of graphene, the dynamic control of threshold power is possible, that allows to actively limit transmitted power for selected or given range of THz frequencies. With a simple multilayer structure based on graphene and polydimethylsiloxane (PDMS) polymer, we show that through appropriate design of nonlinear HMM structure, new functionalities of hyperbolic metamaterials as tunable self-limiting terahertz power limiter and/or controllable laser noise suppressor are possible. We believe that the proposed HMM-based power limiter could serve as a key component of contemporary and future THz systems.

Our work is organized in the following manner: the next section presents the theoretical background for our analysis, including the description of the linear and nonlinear graphene conductivity as well as the transfer matrix method (TMM), suitable for modelling propagation and transmittance/reflectance characteristics in multilayered structures. The third section is dedicated to the analysis and discussion of obtained results, which includes analysis structural and geometry parameters, which are important in design process, as well as verification of spectral and directional properties of postulated optical applications. Finally, the last section contains summary and highlights of the performed investigations.

## II. THEORY

In our analysis, we consider a nonlinear HMM structure consisting of subsequent ultrathin graphene-dielectric stacks, with basic cell is composed of mono- or multi-layer graphene and PDMS dielectric layer, deposited on a thick transparent substrate, see Fig. 1

This section contains description of analytical models of considered materials, namely graphene and polydimethylsiloxane (PDMS) polymer. Additionally, transfer matrix method, which

has been employed to describe propagation and to calculate transmittance and reflectance characteristics of the considered optical system, has been presented in this section.

### A. Material Models

In THz spectral range graphene's permittivity may be described with a Drude type analytical expression

$$\varepsilon_g(\omega, \mu_c) = 1 - j \frac{\sigma(\omega, \mu_c)}{\omega \varepsilon_0 t_g}, \quad (1)$$

where  $\omega$  is the pulsation of incident radiation,  $\varepsilon_0$  is the permittivity of vacuum,  $t_g$  is the thickness of graphene layer, which equals 0.35 nm for a monolayer, and  $\sigma(\omega, \mu_c) = \sigma_{\text{intra}}^L + \sigma_{\text{inter}}^L + |E_0|^2 \cdot \sigma_{\text{intra}}^{NL}$  is the conductivity of graphene sheet, that consists of three components in total, namely linear intra-  $\sigma_{\text{intra}}^L$  and inter-band  $\sigma_{\text{inter}}^L$  terms as well as Kerr-like nonlinear conductivity  $\sigma_{\text{intra}}^{NL}$  in the intraband regime, that is proportional to the square of the amplitude of impinging wave  $E_0$  [58], [59], [60].

In the absence of static magnetic field and weak spatial dispersion, which is true for unshaped graphene sheets, linear terms of graphene's conductivity can be approximated as follows [61]:

$$\sigma_{\text{intra}}^L = -j \frac{e^2 k_B T}{\pi \hbar^2 (\omega - 2j/\tau)} \left( \frac{\mu_c}{k_B T} + 2 \ln \left( e^{-\frac{\mu_c}{k_B T}} + 1 \right) \right), \quad (2)$$

$$\sigma_{\text{inter}}^L = \frac{-j e^2}{4\pi \hbar} \ln \left( \frac{2|\mu_c| - (\omega - 2j/\tau) \hbar}{2|\mu_c| + (\omega - 2j/\tau) \hbar} \right), \quad (3)$$

where  $\omega$  is angular frequency of the incident electromagnetic wave,  $\mu_c$  is the chemical potential of graphene,  $e$  is the elementary charge,  $T = 300$  K is ambient temperature,  $\tau = 5e-13$  is the phenomenological scattering rate,  $k_B$  is Boltzmann constant and  $\hbar$  is the Planck constant. According to the recent experimental studies [62], [63], two-photon absorption in graphene is negligible, thus nonlinear conductivity may be presented in the following form [59], [58]:

$$\sigma_{\text{intra}}^{NL} = -j \frac{3}{32} \frac{e^2}{\pi \hbar} \frac{(e v_F)^2}{\mu_c \omega^3}, \quad (4)$$

where  $v_F = 10^6$  m/s is the Fermi velocity [64]. It is worth to underline that, since the nonlinear term  $\sigma_{\text{intra}}^{NL}$  is purely imaginary and negative, it reveals self-focusing character. Moreover, due to the fact that, 2nd order nonlinearity in graphene has been demonstrated to be significant under certain conditions [65], [66], [67], it can be expected that the overall optical properties will be strongly affected by it.

In general, the chemical potential of graphene may be controlled via passive factors, such as chemical doping, e.g., exposure to NO<sub>2</sub> gas [68], or active stimuli, such as temperature, magnetic field and static voltage bias [69], [70], which can be dynamically tuned. In this work, we employ voltage bias as a factor controlling chemical potential of graphene. The relationship between applied external voltage and chemical potential may be described via Dirac-cone approximation [71]:

$$|\mu_c| = \hbar v_F \sqrt{\pi |a_0 (V_g - V_{\text{dirac}})|}, \quad (5)$$

where  $V_g$  is the applied external voltage,  $V_{\text{dirac}}$  is the offset bias voltage reflecting graphene's doping or impurities, and  $a_0 = 9 \times 10^{16} \text{ m}^{-1}\text{V}^{-1}$  is an empirical constant [72].

The dielectric material constituting the multilayer metamaterial has been described as a transparent material with purely real electric permittivity ( $\epsilon_{\text{PDMS}} \approx 1.78$ ), which corresponds to properties of polydimethylsiloxane (PDMS) within 0.2–4 THz [73]. Finally, the optical parameters of substrate considered in this paper has been also based on THz properties of PDMS, which is highly transparent within considered spectral range.

### B. Transfer Matrix Method

In this work, we use approach to transfer matrix method proposed by Katsidis and Siapakas [74]. According to [74], the amplitudes of electric field in each layer composing a multilayer structure are related to each other by product of  $2 \times 2$  matrices in sequence. In the considered method, each layer is described with a propagation matrix  $\mathbf{P}$ , which connects the field amplitudes at the left- and right-hand side of the layer, and for the  $(j-1)$ -th layer may be written as follows:

$$\mathbf{P}_{j-1} = \begin{bmatrix} \exp(i\delta_{j-1}) & 0 \\ 0 & \exp(-i\delta_{j-1}) \end{bmatrix}, \quad (6)$$

where  $\delta_{j-1} = 2\pi k_0 n_{j-1} d_{j-1} \cos\theta_{j-1}$  is the phase thickness of the  $(j-1)$ -th layer with  $k_0$  being freespace wavevector,  $n_{j-1}$  is refractive index of the layer,  $d_{j-1}$  is layer physical thickness, and  $\theta_{j-1}$  is the angle of incidence. The considered multilayer optical system also includes multiple interfaces between layers and/or surrounding media, which are represented with product of dynamical matrices  $\mathbf{D}^{-1}\mathbf{D}$ , that for  $(j-1)$ -th and  $j$ -th layers can be described as follows:

$$\mathbf{D}_{j-1}^{-1} \mathbf{D}_j = \frac{1}{t_{j-1,j}} \begin{bmatrix} 1 & r_{j-1,j} \\ r_{j-1,j} & 1 \end{bmatrix}, \quad (7)$$

where  $r_{j-1,j}$  and  $t_{j-1,j}$  are the complex Fresnel reflection and transmission amplitude coefficients, respectively. It is noteworthy that the form of the matrix product  $\mathbf{D}_{j-1}^{-1}\mathbf{D}_j$  is invariant of light polarization.

Thus, an optical system composed of  $2N$  alternating layers, that are deposited on a substrate and surrounded with air, may be described via following transfer matrix

$$\mathbf{T} = \mathbf{D}_{\text{air}}^{-1} \mathbf{D}_1 \mathbf{P}_1 \mathbf{D}_1^{-1} \dots \mathbf{D}_{2N} \mathbf{P}_{2N} \mathbf{D}_{2N}^{-1} \mathbf{D}_{\text{sub}} \mathbf{P}_{\text{sub}} \mathbf{D}_{\text{sub}}^{-1} \mathbf{D}_{\text{air}}, \quad (8)$$

where  $\mathbf{D}_{\text{air}}$ ,  $\mathbf{D}_{\text{sub}}$ ,  $\mathbf{P}_{\text{sub}}$ , are dynamical and propagation matrices of substrate and air surrounding the complete structure. Additionally, under the assumption that substrate is thick enough for light to not maintain coherence along the layer, it is possible to formulate intensity transfer matrix, which connects the intensities of field at the left- and right-side of the structure [74]

$$\begin{bmatrix} \mathbf{E}_{\text{int},LHS}^+ \\ \mathbf{E}_{\text{int},LHS}^- \end{bmatrix} = \mathbf{T}^{\text{int}} \begin{bmatrix} \mathbf{E}_{\text{int},RHS}^+ \\ \mathbf{E}_{\text{int},RHS}^- \end{bmatrix} \\ = \begin{bmatrix} T_{11}^{\text{int}} & T_{12}^{\text{int}} \\ T_{21}^{\text{int}} & T_{22}^{\text{int}} \end{bmatrix} \begin{bmatrix} \mathbf{E}_{\text{int},RHS}^+ \\ \mathbf{E}_{\text{int},RHS}^- \end{bmatrix}, \quad (9)$$

where

$$\mathbf{T}^{\text{int}} = (\mathbf{D}_{\text{air}}^{-1} \mathbf{D}_1 \mathbf{P}_1 \mathbf{D}_1^{-1} \dots \mathbf{D}_{2N} \mathbf{P}_{2N} \mathbf{D}_{2N}^{-1} \mathbf{D}_{\text{sub}})^2 \cdot \mathbf{P}_{\text{sub}}^2 \cdot (\mathbf{D}_{\text{sub}}^{-1} \mathbf{D}_{\text{air}})^2. \quad (10)$$

Finally, the transmittance and reflectance of the system are given by the elements of the intensity transfer matrix

$$T_{\text{coef}} = \frac{1}{T_{11}^{\text{int}}}, \quad (11)$$

and

$$R_{\text{coef}} = \frac{T_{21}^{\text{int}}}{T_{11}^{\text{int}}}. \quad (12)$$

It is worth noting that, since the input and output medium is air, the transmittance power coefficient does not require equalization of impedances.

### III. RESULTS

Ideally, an operational power limiter should completely (or partially) cut off transmission of signal when optical power reaches and exceeds a certain threshold. Such functionality is required to avoid damaging (often permanently) sensitive optoelectronic components, e.g., photodiode. In this paper, we investigate possibility of employing a metamaterial structure to act as an efficient optical power limiter. For this purpose, we analyze a metamaterial structure composed of  $N$  basic cells of mono- or multi-layer graphene ( $N_g$  is the number of multilayers) and PDMS dielectric layer, deposited on 2 mm thick PDMS substrate, see Fig. 1. It is worth to underline that, since in our analysis we primarily study influence of laser power over the transmittance of the proposed system, the considered range of light intensity (up to 25 MW/cm<sup>2</sup>) is achievable with a 0.8W THz laser focused on area of 1 cm<sup>2</sup>, which is conceivable with contemporary laser technology [75], [76], [77]. Thus, for better insight, we use local intensity of electric field in our analysis, which is an equivalent yet more intuitive representation than electric field amplitude. For a monochromatic wave travelling in vacuum, the local intensity may be calculated as follows [78]

$$I = \frac{c_0 \epsilon_0}{2} |E_0|^2, \quad (13)$$

where  $c_0$  is the light speed in vacuum.

In the following section, we have presented sets of transmittance and reflectance characteristics of the considered optical system, see Fig. 1, that will allow us to assess the possibility of employing hyperbolic metamaterial as an optical power limiter. All demonstrated characteristics have been acquired with the help models and TMM approach presented in the Section II.

#### A. Designing System Based on Nonlinear HMM

Firstly, we need to determine whether considered hyperbolic metamaterial transmits THz signal for low power radiation, i.e., linear regime  $I = 0$  (on-state). For this purpose, we have determined a set of spectral characteristics illustrating influence of different structural and geometrical parameters on transmittance, namely: thickness of dielectric layer  $t_{\text{PDMS}}$  (Fig. 2(a)) and

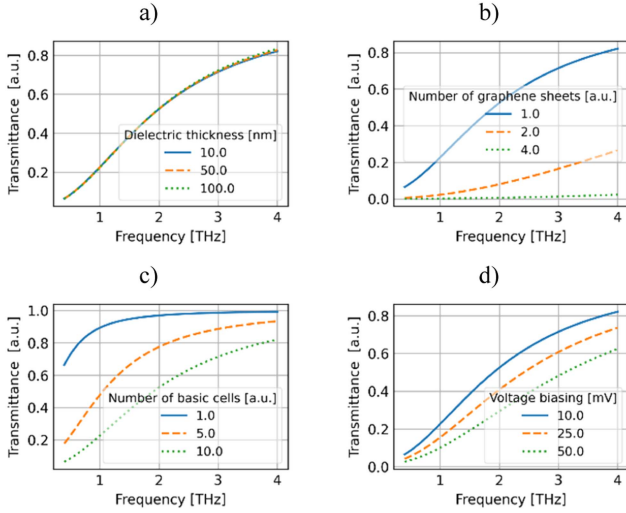


Fig. 2. Transmittance vs. frequency for various values of dielectric thickness (a), number of graphene monolayers (b), number of basic cells (c) and voltage biasing (d).

number of graphene monolayers in the unit cell  $N_g$  (Fig. 2(b)), number of unit cells in the structure  $N$  (Fig. 2(c)), as well as biasing voltage of graphene sheets  $V_g$  (Fig. 2(d)). Unless explicitly stated otherwise in the plot legend, the characteristics have been calculated for a set of fixed parameters:  $t_{\text{PDMS}} = 10$  nm,  $N_g = 1$ ,  $N = 10$  and  $V_g = 10$  mV.

It can be observed that thickness of the dielectric layer in the basic cell has negligible influence on the overall transmittance in the considered spectral range, see Fig. 2(a), which is caused by the fact that the dielectric material is transparent within THz range [73] and optical path length is too small for interference effects to occur. Due to that, the fabrication process is less prone to factors influencing nucleation and growth of the dielectric layer, which significantly increase feasibility of the proposed multilayer structure. On the other hand, increasing a number of graphene monolayers in the basic cell leads not only to higher complexity of fabrication process, but also significantly decreases transmittance for whole considered spectrum, see Fig. 2(b). Hence, to provide high level of transmittance for low power signal, it is beneficial to limit number of graphene monolayers in the basic cell. Similarly, reducing number of basic cells may also lead to lower technological complexity and higher transmission of low power optical signal, see Fig. 2(c). Finally, the voltage biasing of graphene may be applied as a dynamically controlled parameter, which adjusts level of transmittance for low power signal. Typically, it is preferred to achieve high transparency, thus maintaining low voltage biasing would be more suitable, i.e.,  $V_g = 10$  mV, see Fig. 2(d).

An elevated level of transparency of considered structure for low power THz signal can be achieved for a structure consisted of a one basic cell  $N = 1$  consisted of PDMS layer of arbitrary thickness and a single graphene monolayer  $N_g = 1$ , which is biased with low value of external voltage, e.g.,  $V_g = 10$  mV.

Now, let us investigate influence of those parameters on power limiter functionality. For this purpose, we have calculated four sets of characteristics illustrating transmittance as a function of

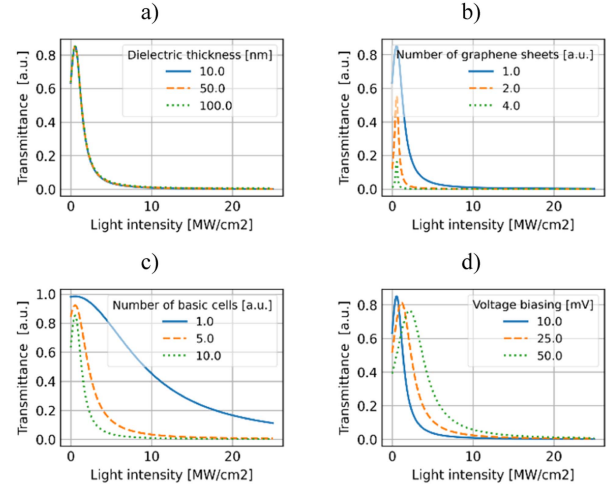


Fig. 3. Transmittance vs. light intensity for various values of dielectric thickness (a), number of graphene monolayers (b), number of basic cells (c) and voltage biasing (d).

light intensity for a signal of a sample frequency  $f = 2.5$  THz, which has been chosen arbitrary from the considered spectral range, see Fig. 3(a)–(d). Again, the characteristics have been plotted for different thickness of dielectric layer  $t_{\text{PDMS}}$  (Fig. 3(a)) and number of graphene monolayers in the unit cell  $N_g$  (Fig. 3(b)), number of unit cells in the structure  $N$  (Fig. 3(c)), as well as biasing voltage of graphene sheets  $V_g$  (Fig. 3(d)). For the comparative purpose, the characteristics have been calculated for the same set of fixed parameters as in the case of low power signal:  $t_{\text{PDMS}} = 10$  nm,  $N_g = 1$ ,  $N = 10$  and  $V_g = 10$  mV, unless explicitly stated otherwise in the plot legend.

It can be observed that power limiter functionality, i.e., signal transmission inversely proportional to its intensity, may be achieved in the considered class of structures for any combination of parameters, see Fig. 3(a)–(d). Additionally, by proper choice of those parameters, it is possible to shift power threshold, i.e., a value of power intensity for which transmittance is at half maximum, and change the slope of transition between on-state (high transparency for low power signal) and off-state ( $T_{\text{coef}} \approx 0$ ). Again, it can be noticed that thickness of dielectric layer has negligible impact on overall transmission, see Fig. 3(a). Thus, there is no need for precise control of its thickness during manufacturing process. By increasing the number of graphene sheets in the basic cell, it is possible to achieve lower power threshold with higher slope, but transmission level in the on-state is strongly suppressed, see Fig. 3(b). Similar effect may be obtained with increasing the number of the basic cells in the structure, see Fig. 3(c). It is worth to underline, however, that both methods may substantially complicate the manufacturing process. Finally, the power threshold and slope may be dynamically adjusted by changing the biasing voltage, see Fig. 3(d). In particular, increasing applied voltage leads to higher power threshold and less steep slope. In general, it can be observed that low value of power threshold coincides with high steepness of the slope, see Fig. 3(a)–(d), which may be beneficial for the considered application. However, for power limiter functionality, it is also advantageous to avoid unnecessary loss

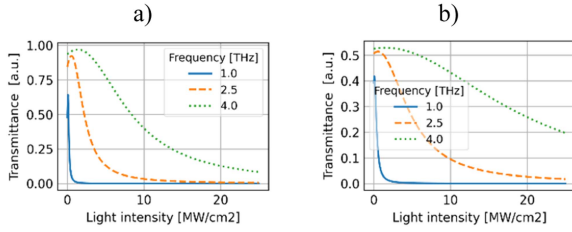


Fig. 4. Transmittance vs. frequency of the signal for a standalone structure suspended in air (a) and deposited on a high-purity Si substrate (b).

of signal in the on-state. Thus, an HMM structure revealing such functionality should be biased with low external voltage, e.g.,  $V_g = 10$  mV. Again, the choice of PDMS layer thickness is arbitrary, due to its low impact on the RT characteristics. On the other hand, the selection of number of basic cells  $N$  and number of graphene monolayers  $N_g$  is characterized by a trade-off between the high level of transparency in the on-state and high steepness of the slope, see Figs. 2(b), (c) and 3(b), (c). Thus, the set of parameters, which will be used in the further analysis and allows the considered optical system to operate in suboptimal condition, has been chosen as follows:  $t_{\text{PDMS}} = 10$  nm,  $N_g = 1$ ,  $N = 10$  and  $V_g = 10$  mV.

For considered class of structure, there is a trade-off between the level of transparency for low-intensity light and the steepness of the transition between on- and off-states as indicated in Figs. 2(a)–(d) and 3(a)–(d). Thus, for a chosen frequency, both of those quantities can be adjusted by selecting appropriate value of voltage biasing and/or number of basic cells. Due to optical loss introduced by graphene, this issue is of paramount importance for light of frequency lower than 2.5 THz. Thus, to avoid unnecessary attenuation, it may be beneficial to reduce the number of basic cells at the cost of slope steepness.

Ideally, the presence of an optical limiter in the optical system should not introduce any insertion loss. In the considered structure, the amount of signal that is lost is determined by the level of transmittance in the on-state, which, due to negligibly small dimensions of the HMM structure in comparison to wavelength considered, is primarily dependent on the impedance mismatch between air and substrate medium, see Fig. 4(a)–(b). In particular, it can be observed that the considered HMM structure, that is “suspended” in the air, reveals much lower insertion loss in comparison to a structure deposited on a high-index Si substrate [79], compare Fig. 4(a) and (b). Thus, employing a suitable anti-reflective coating would further improve the overall performance of the device.

In general, the considered class of structure may efficiently cut-off high power radiation. Moreover, obtaining low power threshold and/or steep slope transition between on- and off-state for a given frequency is possible but requires a proper choice of structural and geometrical parameters of the metamaterial structure, as indicated in the performed analysis.

### B. Optical Power Limiter: Spectral and Directional Properties

Until now, the analysis has been performed for either a single frequency or low optical power. To confirm whether the optical

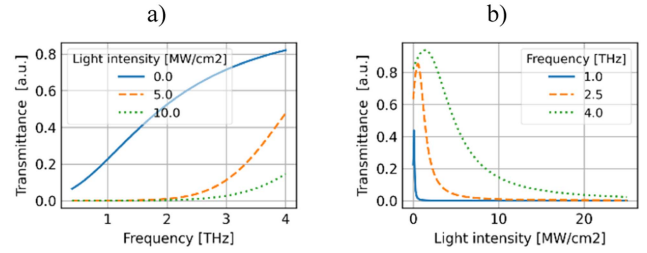


Fig. 5. Transmittance vs. frequency of the signal for various light intensities (a), transmittance vs. light intensity of the signal for different frequencies (b).

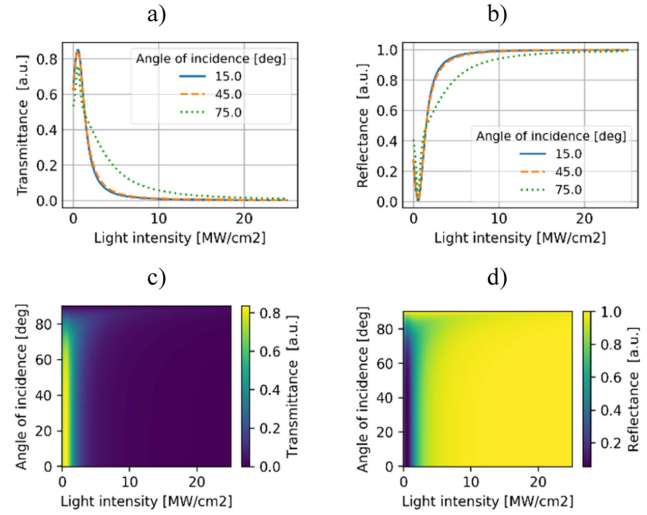


Fig. 6. Transmittance (a) and reflectance (b) vs. light intensity of the signal impinging at different angles. Color plots of transmittance (c) and reflectance (d) vs. light intensity (x-axis) and angle of incidence (y-axis).

power limiter functionality may be obtained within the whole considered spectral range, we have calculated transmittance characteristics for signals of different levels of light intensity and frequencies, see Fig. 5(a)–(b). It is worth to underline that the considered optical system is still based on previously determined set of parameters, i.e.,  $t_{\text{PDMS}} = 10$  nm,  $N_g = 1$ ,  $N = 10$  and  $V_g = 10$  mV, that provides a suboptimal power-limiting performance.

As we can see, increasing light intensity of signal leads to lower transmission within the considered spectral range, see Fig. 5(a). It can be observed that, higher frequency signals reveal higher power threshold, Fig. 5(b). Thus, larger level of power is required to achieve complete cut-off of the signal ( $T_{\text{coef}} \approx 0$ ). Nevertheless, the proposed structure reveals optical power limiter functionality within the considered THz spectral range.

Thus far, we have investigated only transmission of the proposed device solely at normal incidence. To fully validate applicability of the structure, we have also investigated reflectance and transmittance for a 2.5 THz signal impinging at different angles, see Fig. 6(a)–(d).

It can be observed that the desired power-dependent transmittance and reflectance properties of the structure are perfectly

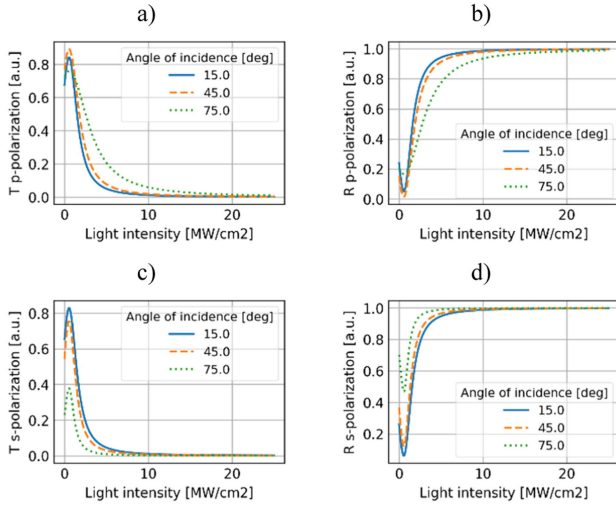


Fig. 7. Transmittance (a,c) and reflectance (b,d) vs. light intensity plotted for different angle of incidence of the signal of various polarization: TE- (a,b) and TM polarization (c,d).

preserved over large angle of incidence, up to  $\theta_{\text{inc}} = 45^\circ$ , see Fig. 6(a)–(d). Additionally, the structure reveals very low absorption  $<1\%$  ( $A_{\text{coef}} \approx 1 - R_{\text{coef}} - T_{\text{coef}} < 0.01$ ) for light intensity larger than  $I > 4.5 \text{ MW/cm}^2$ . Thus, the proposed structure efficiently reflects signal of excessive power, instead of dissipating/absorbing impinging radiation, which allows to avoid damaging the structure.

Typically, an HMM structure reveals strong anisotropy, which may deteriorate functionality of the proposed structure in case of polarized light. To investigate that phenomenon, a set of characteristics illustrating power-dependent transmittance and reflectance for TE and TM-polarized waves impinging at different angles have been calculated, see Fig. 7(a)–(d).

Again, substantial alteration of power limiter functionality for both polarizations occurs only for large angle of incidence, i.e., in case of  $\theta_0 = 75^\circ$  power threshold is shifted for TE-polarized waves, see Fig. 7(a) and (b), while overall level of transmittance is much lower for light of TM polarization, see Fig. 7(c) and (d). However, for smaller angles, i.e.,  $\theta_0 < 45^\circ$ , the desired performance is still well preserved. Thus, the proposed structure may be considered as polarization invariant, up to  $\theta_0 < 45^\circ$  angle of incidence, which extends applicability of the considered system to sources of polarized radiation.

### C. Two Modes of Operation: Tunable Optical Power Limiter and Laser Noise Suppressor

Until now, it has been demonstrated that the considered hyperbolic metamaterial structure based on graphene reveals power-dependent transmittance and reflectance within 0.4–4 THz spectral range and wide angle of incidence, up to  $\theta_0 < 45^\circ$ . For the same set of structural parameters, i.e.,  $t_{\text{PDMS}} = 10 \text{ nm}$ ,  $N_g = 1$  and  $N = 10$ , this behavior allows us to employ the considered structure as an optical power limiter, that transmits signal of power below certain power threshold and rejects signals of higher power, see 8(a). What is more, the proposed structure cuts off the excessive power by reflecting radiation rather than

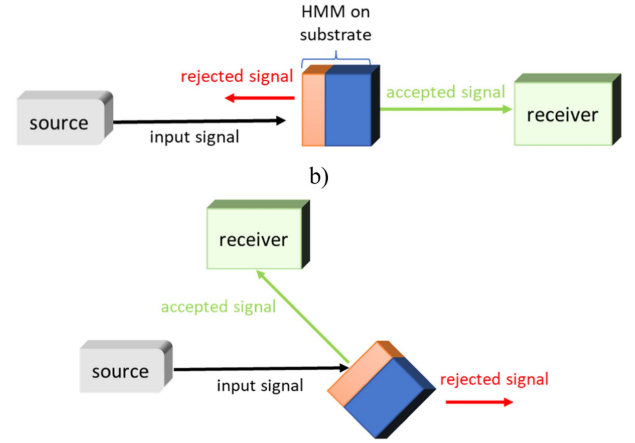


Fig. 8. Proposed optical setup schemes for operation as a power limiter (a) and a laser noise suppressor (b).

absorbing it, which limits possible damage of the structure, i.e., the proposed structure perfectly ( $R_{\text{coef}} \approx 1$ ) reflects radiation of higher intensity ( $I > 10 \text{ MW/cm}^2$ ), see Fig. 7(a)–(d). The efficient power-dependent reflectance also creates opportunity to employ that structure as a mirror reflecting only signal of high power, see Fig. 8(b). In the considered optical setup, the same HMM structure would “reject” low power signal by transmitting away from the receiver. On the other hand, optical signal with power above given threshold will be “accepted” by redirecting (reflecting) towards the receiver, see Fig. 8(a). Due to that, the considered structure can be employed in applications requiring rejection of low power optical signal, such as elimination of excessive noise that is generated in a laser operating below lasing (power) threshold.

Additionally, due to the sensitivity of graphene to external static bias, it is possible to dynamically adjust the power threshold of a single structure by changing voltage biasing. To illustrate that functionality, we have calculated characteristics of power-dependent transmittance and reflectance for a single structure operating under different values of applied voltage, see Fig. 9(a)–(b). In particular, it can be observed that for the considered structure, it is possible to shift the power threshold from  $I \approx 3 \text{ MW/cm}^2$  to  $I \approx 8 \text{ MW/cm}^2$ .

Therefore, the proposed structure may operate in transmission mode, see Figs. 8(a), 9(a) and (c), as tunable optical power limiter that reflects signal of power exceeding certain power threshold or in reflection mode, see Figs. 8(b), 9(b) and (d), as a laser noise suppressor, that rejects signal below chosen power (e.g., lasing) threshold. It is worth to reiterate, that the crucial operational parameters, such as transmission for low-intensity light, threshold intensity and slope steepness, may be further optimized for selected frequency or range of frequencies by choice appropriate number of basic cells, graphene monolayers or applied voltage.

### D. Feasibility Analysis

It is worth to underline, that considered constituent materials, i.e., graphene and PDMS, are chosen as an example to

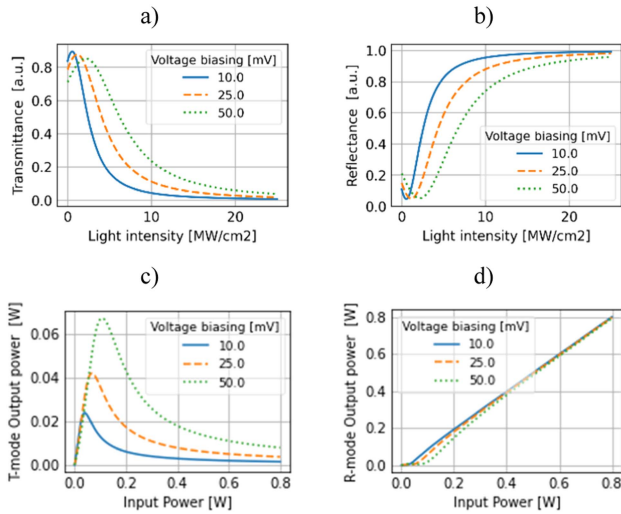


Fig. 9. Transmittance (a) and reflectance (b) vs. light intensity of the signal for various values of voltage biasing. Output power for the considered structure working in T- (c) and R-mode (d) plotted vs. input power.

demonstrate more general functionality of nonlinear HMM and, thus, may be substituted with materials revealing similar optical properties within chosen spectral range and/or lower optical absorption. Moreover, both considered materials, as long as their characteristics dimensions are larger than the considered wavelength, may be considered local and isotropic. However, to better realize the potential of the presented device, it is purposeful to shortly discuss its feasibility. It is worth noting, that similar multilayer stacks of graphene-based structures have been successfully fabricated and their tunability have been proven experimentally [80], [81]. The graphene monolayers can be deposited on Cu substrate with the help of CVD [81] and then mechanically transferred onto dielectric layer with the use of standard or acetic acid method [82]. Subsequent basic cells may be deposited in a step-by-step manner. It is also worth noting that, application of graphene as a plasmonic material, allows us to obtain tunability of the complete HMM structure by controlling its chemical potential with change of temperature and static magnetic or electric field [69], [70]. In the considered case of voltage-dependent tunability, additional layers acting as transparent electrodes at top and bottom of the HMM structure are required. Thus, considered HMM structure with electrodes is electrically equivalent to a double gate plate capacitor. The speed of tuning is limited by charge accumulation effect in the capacitor, i.e., the  $\tau = RC$  time constant of the capacitor, which, for a structure constructed of  $N = 10$  basic cells with monolayer graphene and 10 nm dielectric layer and  $A \approx 1 \text{ cm}^2$  electrode area, is of the order of several nanoseconds.

#### IV. CONCLUSION

Over the course of this paper, we have demonstrated the possibility of employing graphene-based hyperbolic metamaterial as a tunable optical power limiter (transmission mode) and/or controllable laser noise suppressor (reflection mode) operating in THz spectral range, which is of paramount importance in

optical system and components, that are susceptible to excessive signal power or noise. The proposed class of structures, due to voltage sensitivity of graphene, also offers a possibility of dynamic tuning its properties. Another significant advantage of graphene-based structure is simultaneous existence of plasmonic and strong nonlinear response within THz spectral range, which is crucial in the considered application. Due to that, the power threshold of a single structure may be adjusted to desired value by applying appropriate voltage. Moreover, we have presented that nonlinear hyperbolic metamaterials reveal considered functionalities over 0.2–4 THz band and wide acceptance cone, up to  $\theta_0 = 45^\circ$  angle of incidence, while maintaining high power transmission in the on-state, which may be considered as a significant improvement in comparison with conventional resonator-based solution [15], [57]. Within our analysis we have also indicated that, crucial parameters, such as power threshold and steepness of the slope between on- and off-state, may be further adjusted by proper choice of structural and geometrical parameters of considered optical system structure, while maintaining high transmittance level in the on-state and resilience to the angle of incidence. We strongly believe that, due to relatively low sensitivity to precise layer deposition, broadband spectral operation range and low absorption, the proposed class of nonlinear metamaterials may be successfully employed in practical THz applications requiring optical power limiting.

#### REFERENCES

- [1] P. Jepsen, D. Cooke, and M. Koch, "Terahertz spectroscopy and imaging—Modern techniques and applications," *Laser Photon. Rev.*, vol. 5, no. 1, pp. 124–166, 2011, doi: [10.1002/lpor.201000011](https://doi.org/10.1002/lpor.201000011).
- [2] C. Jansen et al., "Terahertz imaging: Applications and perspectives," *Appl. Opt.*, vol. 49, no. 19, pp. E48–E57, Jul. 2010, doi: [10.1364/AO.49.000E48](https://doi.org/10.1364/AO.49.000E48).
- [3] W. Xu, L. Xie, and Y. Ying, "Mechanisms and applications of terahertz metamaterial sensing: A review," *Nanoscale*, vol. 9, no. 37, pp. 13864–13878, Sep. 2017, doi: [10.1039/C7NR03824K](https://doi.org/10.1039/C7NR03824K).
- [4] O. Paul, R. Beigang, and M. Rahm, "Highly selective terahertz bandpass filters based on trapped mode excitation," *Opt. Exp.*, vol. 17, no. 21, pp. 18590–18595, Oct. 2009, doi: [10.1364/OE.17.018590](https://doi.org/10.1364/OE.17.018590).
- [5] A. Andryieuski and A. V. Lavrinenko, "Graphene metamaterials based tunable terahertz absorber: Effective surface conductivity approach," *Opt. Exp.*, vol. 21, no. 7, pp. 9144–9155, Apr. 2013, doi: [10.1364/OE.21.009144](https://doi.org/10.1364/OE.21.009144).
- [6] J. Federici and L. Moeller, "Review of terahertz and subterahertz wireless communications," *J. Appl. Phys.*, vol. 107, no. 11, Jun. 2010, Art. no. 111101, doi: [10.1063/1.3386413](https://doi.org/10.1063/1.3386413).
- [7] S. Atakaramians, A. V. S., T. M. Monro, and D. Abbott, "Terahertz dielectric waveguides," *Adv. Opt. Photon.*, vol. 5, no. 2, pp. 169–215, Jun. 2013, doi: [10.1364/AOP.5.000169](https://doi.org/10.1364/AOP.5.000169).
- [8] H. A. Hafez et al., "Intense terahertz radiation and their applications," *J. Opt.*, vol. 18, no. 9, Sep. 2016, Art. no. 093004, doi: [10.1088/2040-8978/18/9/093004](https://doi.org/10.1088/2040-8978/18/9/093004).
- [9] A. E. Siegman, "Nonlinear optical effects: An optical power limiter," *Appl. Opt.*, vol. 1, no. S1, pp. 127–132, Jan. 1962, doi: [10.1364/AO.1.S1.000127](https://doi.org/10.1364/AO.1.S1.000127).
- [10] D. J. Hagan, S. Guha, E. W. Van Stryland, M. J. Soileau, and Y. Y. Wu, "Self-protecting semiconductor optical limiters," *Opt. Lett.*, vol. 13, no. 4, pp. 315–317, Apr. 1988, doi: [10.1364/OL.13.000315](https://doi.org/10.1364/OL.13.000315).
- [11] R. C. Hollins, "Materials for optical limiters," *Curr. Opin. Solid State Mater. Sci.*, vol. 4, no. 2, pp. 189–196, Apr. 1999, doi: [10.1016/S1359-0286\(99\)00009-1](https://doi.org/10.1016/S1359-0286(99)00009-1).
- [12] B. Y. Soon, J. W. Haus, M. Scalora, and C. Sibilia, "One-dimensional photonic crystal optical limiter," *Opt. Exp.*, vol. 11, no. 17, Aug. 2003, Art. no. 2007, doi: [10.1364/OE.11.002007](https://doi.org/10.1364/OE.11.002007).
- [13] M. Danaie and H. Kaatuzian, "Design and simulation of an all-optical photonic crystal AND gate using nonlinear Kerr effect," *Opt. Quantum Electron.*, vol. 44, no. 1/2, pp. 27–34, May 2012, doi: [10.1007/s11082-011-9527-y](https://doi.org/10.1007/s11082-011-9527-y).

- [14] A. P. Menezes, S. Raghavendra, A. Jayarama, H. P. Sarveshwara, and S. M. Dharmaprakash, "Structural, thermal, linear and nonlinear optical studies of an organic optical limiter based on reverse saturable absorption," *J. Mol. Struct.*, vol. 1119, pp. 167–176, Sep. 2016, doi: [10.1016/j.molstruc.2016.04.052](https://doi.org/10.1016/j.molstruc.2016.04.052).
- [15] J. Huang, Y. Lu, L. Zhou, F. Xu, and D. Zuo, "Design of photonic crystal nonlinear laser power limiter based on topological edge states and optical Kerr effect," *Opt. Exp.*, vol. 28, no. 8, pp. 12080–12092, Apr. 2020, doi: [10.1364/OE.390297](https://doi.org/10.1364/OE.390297).
- [16] Z. Liu, B. Zhang, and Y. Chen, "Recent Progress in two-dimensional nanomaterials for laser protection," *Chemistry*, vol. 1, no. 1, pp. 17–43, Jan. 2019, doi: [10.3390/chemistry1010004](https://doi.org/10.3390/chemistry1010004).
- [17] R. Gadhwal, P. Kaushik, and A. Devi, "A review on the development of optical limiters from homogeneous to reflective 1-D photonic crystal structures," *Opt. Laser Technol.*, vol. 141, Sep. 2021, Art. no. 107144, doi: [10.1016/j.optlastec.2021.107144](https://doi.org/10.1016/j.optlastec.2021.107144).
- [18] R. Gadhwal, P. Kaushik, and A. Devi, "A review on 1D photonic crystal based reflective optical limiters," *Crit. Rev. Solid State Mater. Sci.*, vol. 48, no. 1, pp. 93–111, Jan. 2023, doi: [10.1080/10408436.2022.2041394](https://doi.org/10.1080/10408436.2022.2041394).
- [19] R. Kersting, G. Strasser, and K. Unterrainer, "Terahertz phase modulator," *Electron. Lett.*, vol. 36, no. 13, pp. 1156–1158, Jun. 2000, doi: [10.1049/el:20000837](https://doi.org/10.1049/el:20000837).
- [20] W. J. Padilla, A. J. Taylor, C. Highstrete, M. Lee, and R. D. Averitt, "Dynamical electric and magnetic metamaterial response at terahertz frequencies," *Phys. Rev. Lett.*, vol. 96, no. 10, Mar. 2006, Art. no. 107401, doi: [10.1103/PhysRevLett.96.107401](https://doi.org/10.1103/PhysRevLett.96.107401).
- [21] H.-T. Chen et al., "Experimental demonstration of frequency-agile terahertz metamaterials," *Nature Photon.*, vol. 2, no. 5, pp. 295–28, May 2008, doi: [10.1038/nphoton.2008.52](https://doi.org/10.1038/nphoton.2008.52).
- [22] B. Sensale-Rodriguez et al., "Unique prospects for graphene-based terahertz modulators," *Appl. Phys. Lett.*, vol. 99, no. 11, Sep. 2011, Art. no. 113104, doi: [10.1063/1.3636435](https://doi.org/10.1063/1.3636435).
- [23] N. K. Grady et al., "Terahertz metamaterials for linear polarization conversion and anomalous refraction," *Science*, vol. 340, no. 6138, pp. 1304–1307, Jun. 2013, doi: [10.1126/science.1235399](https://doi.org/10.1126/science.1235399).
- [24] H. Tao et al., "A metamaterial absorber for the terahertz regime: Design, fabrication and characterization," *Opt. Exp.*, vol. 16, no. 10, pp. 7181–7188, May 2008, doi: [10.1364/OE.16.007181](https://doi.org/10.1364/OE.16.007181).
- [25] R. Alaei, M. Farhat, C. Rockstuhl, and F. Lederer, "A perfect absorber made of a graphene micro-ribbon metamaterial," *Opt. Exp.*, vol. 20, no. 27, pp. 28017–28024, Dec. 2012, doi: [10.1364/OE.20.028017](https://doi.org/10.1364/OE.20.028017).
- [26] H.-T. Chen et al., "Ultrafast optical switching of terahertz metamaterials fabricated on ErAs/GaAs nanoisland superlattices," *Opt. Lett.*, vol. 32, no. 12, pp. 1620–1622, Jun. 2007, doi: [10.1364/OL.32.001620](https://doi.org/10.1364/OL.32.001620).
- [27] X. Zhao, L. Zhu, C. Yuan, and J. Yao, "Reconfigurable hybrid metamaterial waveguide system at terahertz regime," *Opt. Exp.*, vol. 24, no. 16, pp. 18244–18251, Aug. 2016, doi: [10.1364/OE.24.018244](https://doi.org/10.1364/OE.24.018244).
- [28] J. Zhang and D. Grischkowsky, "Waveguide terahertz time-domain spectroscopy of nanometer water layers," *Opt. Lett.*, vol. 29, no. 14, pp. 1617–1619, Jul. 2004, doi: [10.1364/OL.29.001617](https://doi.org/10.1364/OL.29.001617).
- [29] A. Howes et al., "Optical limiting based on Huygens' metasurfaces," *Nano Lett.*, vol. 20, no. 6, pp. 4638–4644, Jun. 2020, doi: [10.1021/acs.nanolett.0c01574](https://doi.org/10.1021/acs.nanolett.0c01574).
- [30] F. Wu, X. Yu, A. Panda, and D. Liu, "Terahertz angle-independent photonic bandgap in a one-dimensional photonic crystal containing InSb-based hyperbolic metamaterials," *Appl. Opt.*, vol. 61, no. 26, pp. 7677–7684, Sep. 2022, doi: [10.1364/AO.470923](https://doi.org/10.1364/AO.470923).
- [31] D. Liu et al., "High-quality resonances in terahertz composite slabs based on metal gratings," *J. Opt.*, vol. 24, no. 10, Oct. 2022, Art. no. 105103, doi: [10.1088/2040-8986/ac9002](https://doi.org/10.1088/2040-8986/ac9002).
- [32] C. Rizza, A. Ciattoni, E. Spinozzi, and L. Columbo, "Terahertz active spatial filtering through optically tunable hyperbolic metamaterials," *Opt. Lett.*, vol. 37, no. 16, pp. 3345–3347, Aug. 2012, doi: [10.1364/OL.37.003345](https://doi.org/10.1364/OL.37.003345).
- [33] X. Zhou, X. Yin, T. Zhang, L. Chen, and X. Li, "Ultrabroad terahertz bandpass filter by hyperbolic metamaterial waveguide," *Opt. Exp.*, vol. 23, no. 9, pp. 11657–11664, May 2015, doi: [10.1364/OE.23.011657](https://doi.org/10.1364/OE.23.011657).
- [34] K. V. Sreekanth et al., "A terahertz Brewster switch based on superconductor hyperbolic metamaterial," *J. Appl. Phys.*, vol. 128, no. 17, Nov. 2020, Art. no. 173106, doi: [10.1063/5.0025925](https://doi.org/10.1063/5.0025925).
- [35] M. Pourmand and P. K. Choudhury, "Nanostructured strontium titanate perovskite hyperbolic metamaterial supported tunable broadband THz Brewster modulator," *IEEE Trans. Nanotechnol.*, vol. 21, pp. 586–591, 2022, doi: [10.1109/TNANO.2022.3210111](https://doi.org/10.1109/TNANO.2022.3210111).
- [36] J. Liu et al., "Biaxial hyperbolic metamaterial THz broadband absorber utilizing anisotropic two-dimensional materials," *Results Phys.*, vol. 22, Mar. 2021, Art. no. 103818, doi: [10.1016/j.rinp.2021.103818](https://doi.org/10.1016/j.rinp.2021.103818).
- [37] L. Zhang et al., "Tunable bulk polaritons of graphene-based hyperbolic metamaterials," *Opt. Exp.*, vol. 22, no. 11, pp. 14022–14030, Jun. 2014, doi: [10.1364/OE.22.014022](https://doi.org/10.1364/OE.22.014022).
- [38] H. T. Yan, W. Feng, Z. Liu, and J. C. Cao, "Voltage-adjustable terahertz hyperbolic metamaterial based on graphene and doped silicon," *Amer. Inst. Phys. Adv.*, vol. 9, no. 1, Jan. 2019, Art. no. 015108, doi: [10.1063/1.5063309](https://doi.org/10.1063/1.5063309).
- [39] R. Ning, S. Liu, H. Zhang, B. Bian, and X. Kong, "Tunable absorption in graphene-based hyperbolic metamaterials for mid-infrared range," *Physica B: Condens. Matter*, vol. 457, pp. 144–148, Jan. 2015, doi: [10.1016/j.physb.2014.09.038](https://doi.org/10.1016/j.physb.2014.09.038).
- [40] D. Lee et al., "Hyperbolic metamaterials: Fusing artificial structures to natural 2D materials," *ELight*, vol. 2, pp. 1–23, Dec. 2022, doi: [10.1186/s43593-021-00008-6](https://doi.org/10.1186/s43593-021-00008-6).
- [41] S. Poorgholam-Khanjari and F. B. Zarrabi, "Reconfigurable Vivaldi THz antenna based on graphene load as hyperbolic metamaterial for skin cancer spectroscopy," *Opt. Commun.*, vol. 480, Feb. 2021, Art. no. 126482, doi: [10.1016/j.optcom.2020.126482](https://doi.org/10.1016/j.optcom.2020.126482).
- [42] B. Jin, T. Guo, L. Zhu, P.-Y. Chen, and C. Argyropoulos, "Tunable THz generation and enhanced nonlinear effects with active and passive graphene hyperbolic metamaterials," *Proc. SPIE*, vol. 11284, 2020, pp. 54–59, doi: [10.1117/1.2544411](https://doi.org/10.1117/1.2544411).
- [43] Y. Ma, Y. Xu, and H.-F. Zhang, "The tailored saturated-unsaturated defect modes obtained by nonlinear threshold light in graphene-based hyperbolic metamaterial," *IEEE J. Sel. Topics Quantum Electron.*, vol. 29, no. 1, Jan./Feb. 2023, Art. no. 5100107, doi: [10.1109/JSTQE.2021.3135881](https://doi.org/10.1109/JSTQE.2021.3135881).
- [44] O. N. Kozina, L. A. Melnikov, and I. S. Nefedov, "A theory for terahertz lasers based on a graphene hyperbolic metamaterial," *J. Opt.*, vol. 22, no. 9, Sep. 2020, Art. no. 095003, doi: [10.1088/2040-8986/aba678](https://doi.org/10.1088/2040-8986/aba678).
- [45] T. Driscoll et al., "Dynamic tuning of an infrared hybrid-metamaterial resonance using vanadium dioxide," *Appl. Phys. Lett.*, vol. 93, no. 2, Jul. 2008, Art. no. 024101, doi: [10.1063/1.2956675](https://doi.org/10.1063/1.2956675).
- [46] A. E. Nikolaenko et al., "Carbon nanotubes in a photonic metamaterial," *Phys. Rev. Lett.*, vol. 104, no. 15, Apr. 2010, Art. no. 153902, doi: [10.1103/PhysRevLett.104.153902](https://doi.org/10.1103/PhysRevLett.104.153902).
- [47] K. Appavoo and R. F. Haglund, "Detecting nanoscale size dependence in VO<sub>2</sub> phase transition using a split-ring resonator metamaterial," *Nano Lett.*, vol. 11, no. 3, pp. 1025–1031, Mar. 2011, doi: [10.1021/nl103842v](https://doi.org/10.1021/nl103842v).
- [48] W. Huang et al., "Optical switching of a metamaterial by temperature controlling," *Appl. Phys. Lett.*, vol. 96, no. 26, Jun. 2010, Art. no. 261908, doi: [10.1063/1.3458706](https://doi.org/10.1063/1.3458706).
- [49] S. Ghafari, M. R. Forouzeshefard, and Z. Vafapour, "Thermo optical switching and sensing applications of an infrared metamaterial," *IEEE Sensors J.*, vol. 20, no. 6, pp. 3235–3241, Mar. 2020, doi: [10.1109/JSEN.2019.2955672](https://doi.org/10.1109/JSEN.2019.2955672).
- [50] Z. Liu et al., "Triple plasmon-induced transparency and optical switch desensitized to polarized light based on a mono-layer metamaterial," *Opt. Exp.*, vol. 29, no. 9, pp. 13949–13959, Apr. 2021, doi: [10.1364/OE.425315](https://doi.org/10.1364/OE.425315).
- [51] S. Xiao et al., "Active metamaterials and metadevices: A review," *J. Phys. D: Appl. Phys.*, vol. 53, no. 50, Dec. 2020, Art. no. 503002, doi: [10.1088/1361-6463/abaced](https://doi.org/10.1088/1361-6463/abaced).
- [52] I. V. Shadrivov, V. A. Fedotov, D. A. Powell, Y. S. Kivshar, and N. I. Zheludev, "Electromagnetic wave analogue of an electronic diode," *New J. Phys.*, vol. 13, no. 3, Mar. 2011, Art. no. 033025, doi: [10.1088/1367-2630/13/3/033025](https://doi.org/10.1088/1367-2630/13/3/033025).
- [53] I. V. Shadrivov, S. K. Morrison, and Y. S. Kivshar, "Tunable split-ring resonators for nonlinear negative-index metamaterials," *Opt. Exp.*, vol. 14, no. 20, pp. 9344–9349, 2006, doi: [10.1364/OE.14.009344](https://doi.org/10.1364/OE.14.009344).
- [54] D. A. Powell, I. V. Shadrivov, Y. S. Kivshar, and M. V. Gorkunov, "Self-tuning mechanisms of nonlinear split-ring resonators," *Appl. Phys. Lett.*, vol. 91, no. 14, Oct. 2007, Art. no. 144107, doi: [10.1063/1.2794733](https://doi.org/10.1063/1.2794733).
- [55] A. Baev, E. P. Furlani, M. Samoc, and P. N. Prasad, "Negative refractivity assisted optical power limiting," *J. Appl. Phys.*, vol. 102, no. 4, Aug. 2007, Art. no. 043101, doi: [10.1063/1.2769144](https://doi.org/10.1063/1.2769144).
- [56] H. R. Seren et al., "Nonlinear terahertz devices utilizing semiconducting plasmonic metamaterials," *Light Sci. Appl.*, vol. 5, no. 5, May 2016, Art. no. e16078, doi: [10.1038/lsa.2016.78](https://doi.org/10.1038/lsa.2016.78).
- [57] E. Makri, T. Kottos, and I. Vitebskiy, "Reflective optical limiter based on resonant transmission," *Phys. Rev. A*, vol. 91, no. 4, Apr. 2015, Art. no. 043838, doi: [10.1103/PhysRevA.91.043838](https://doi.org/10.1103/PhysRevA.91.043838).



- [58] S. A. Mikhailov and K. Ziegler, "Nonlinear electromagnetic response of graphene: Frequency multiplication and the self-consistent-field effects," *J. Phys.: Condens. Matter*, vol. 20, no. 38, Aug. 2008, Art. no. 384204, doi: [10.1088/0953-8984/20/38/384204](https://doi.org/10.1088/0953-8984/20/38/384204).
- [59] H. Nasari and M. S. Abrishamian, "Terahertz bistability and multistability in graphene/dielectric Fibonacci multilayer," *Appl. Opt.*, vol. 56, no. 19, pp. 5313–5322, Jul. 2017, doi: [10.1364/AO.56.005313](https://doi.org/10.1364/AO.56.005313).
- [60] J. S. Gómez-Díaz and J. Perruisseau-Carrier, "Propagation of hybrid transverse magnetic-transverse electric plasmons on magnetically biased graphene sheets," *J. Appl. Phys.*, vol. 112, no. 12, Dec. 2012, Art. no. 124906, doi: [10.1063/1.4769749](https://doi.org/10.1063/1.4769749).
- [61] G. W. Hanson, "Dyadic Green's functions for an anisotropic, non-local model of biased graphene," *IEEE Trans. Antennas Propag.*, vol. 56, no. 3, pp. 747–757, Mar. 2008, doi: [10.1109/TAP.2008.917005](https://doi.org/10.1109/TAP.2008.917005).
- [62] T. Gu et al., "Regenerative oscillation and four-wave mixing in graphene optoelectronics," *Nature Photon.*, vol. 6, no. 8, pp. 554–559, Aug. 2012, doi: [10.1038/nphoton.2012.147](https://doi.org/10.1038/nphoton.2012.147).
- [63] J. D. Cox and F. J. García de Abajo, "Nonlinear graphene nanoplasmonics," *Accounts Chem. Res.*, vol. 52, no. 9, pp. 2536–2547, Sep. 2019, doi: [10.1021/acs.accounts.9b00308](https://doi.org/10.1021/acs.accounts.9b00308).
- [64] Y. Fan, F. Zhang, Q. Zhao, Z. Wei, and H. Li, "Tunable terahertz coherent perfect absorption in a monolayer graphene," *Opt. Lett.*, vol. 39, no. 21, pp. 6269–6272, Nov. 2014, doi: [10.1364/OL.39.006269](https://doi.org/10.1364/OL.39.006269).
- [65] Y. Wang, M. Tokman, and A. Belyanin, "Second-order nonlinear optical response of graphene," *Phys. Rev. B*, vol. 94, no. 19, Nov. 2016, Art. no. 195442, doi: [10.1103/PhysRevB.94.195442](https://doi.org/10.1103/PhysRevB.94.195442).
- [66] S. Wu et al., "Quantum-enhanced tunable second-order optical nonlinearity in bilayer graphene," *Nano Lett.*, vol. 12, no. 4, pp. 2032–2036, Apr. 2012, doi: [10.1021/nl300084j](https://doi.org/10.1021/nl300084j).
- [67] J. L. Cheng, N. Vermeulen, and J. E. Sipe, "DC current induced second order optical nonlinearity in graphene," *Opt. Exp.*, vol. 22, no. 13, pp. 15868–15876, Jun. 2014, doi: [10.1364/OE.22.015868](https://doi.org/10.1364/OE.22.015868).
- [68] H. Liu, Y. Liu, and D. Zhu, "Chemical doping of graphene," *J. Mater. Chem.*, vol. 21, no. 10, pp. 3335–3345, 2011, doi: [10.1039/C0JM02922J](https://doi.org/10.1039/C0JM02922J).
- [69] B. Guo, L. Fang, B. Zhang, and J. R. Gong, "Graphene doping: A review," *Insciences J.*, vol. 1, pp. 80–89, Apr. 2011, doi: [10.5640/insc.010280](https://doi.org/10.5640/insc.010280).
- [70] B. Janaszek, A. Tyszk-Zawadzka, and P. Szczepański, "Tunable graphene-based hyperbolic metamaterial operating in SCLU telecom bands," *Opt. Exp.*, vol. 24, no. 21, pp. 24129–24136, Oct. 2016, doi: [10.1364/OE.24.024129](https://doi.org/10.1364/OE.24.024129).
- [71] M. Liu et al., "A graphene-based broadband optical modulator," *Nature*, vol. 474, no. 7349, pp. 64–67, Jun. 2011, doi: [10.1038/nature10067](https://doi.org/10.1038/nature10067).
- [72] I. V. Iorsh, I. S. Mukhin, I. V. Shadrivov, P. A. Belov, and Y. S. Kivshar, "Hyperbolic metamaterials based on multilayer graphene structures," *Phys. Rev. B*, vol. 87, no. 7, Feb. 2013, Art. no. 075416, doi: [10.1103/PhysRevB.87.075416](https://doi.org/10.1103/PhysRevB.87.075416).
- [73] A. Podzorov and G. Gallot, "Low-loss polymers for terahertz applications," *Appl. Opt.*, vol. 47, no. 18, pp. 3254–3257, Jun. 2008, doi: [10.1364/AO.47.003254](https://doi.org/10.1364/AO.47.003254).
- [74] C. C. Katsidis and D. I. Siapkas, "General transfer-matrix method for optical multilayer systems with coherent, partially coherent, and incoherent interference," *Appl. Opt.*, vol. 41, no. 19, pp. 3978–3987, Jul. 2002, doi: [10.1364/AO.41.003978](https://doi.org/10.1364/AO.41.003978).
- [75] B. S. Williams, S. Kumar, Q. Hu, and J. L. Reno, "High-power terahertz quantum cascade lasers," in *Proc. Conf. Lasers Electro-Opt. Quantum Electron. Laser Sci. Conf.*, 2006, pp. 1–2, doi: [10.1109/CLEO.2006.4628285](https://doi.org/10.1109/CLEO.2006.4628285).
- [76] L. H. Li et al., "Multi-watt high-power THz frequency quantum cascade lasers," *Electron. Lett.*, vol. 53, no. 12, pp. 799–800, Jun. 2017, doi: [10.1049/el.2017.0662](https://doi.org/10.1049/el.2017.0662).
- [77] C. A. Curwen, J. L. Reno, and B. S. Williams, "Terahertz quantum cascade VECSEL with watt-level output power," *Appl. Phys. Lett.*, vol. 113, no. 1, Jul. 2018, Art. no. 011104, doi: [10.1063/1.5033910](https://doi.org/10.1063/1.5033910).
- [78] "Optical intensity," RP Photonics Encyclopedia. RP Photonics Consulting AG. Accessed: Sep. 13, 2022. [Online]. Available: [www.rp-photonics.com](http://www.rp-photonics.com)
- [79] E. J. Wollack, G. Cataldo, K. H. Miller, and M. A. Quijada, "Infrared properties of high-purity silicon," *Opt. Lett.*, vol. 45, no. 17, pp. 4935–4938, Sep. 2020, doi: [10.1364/OL.393847](https://doi.org/10.1364/OL.393847).
- [80] Q. Zhang et al., "Flyweight, superelastic, electrically conductive, and flame-retardant 3D multi-nanolayer graphene/ceramic metamaterial," *Adv. Mater.*, vol. 29, no. 28, Jul. 2017, Art. no. 1605506, doi: [10.1002/adma.201605506](https://doi.org/10.1002/adma.201605506).
- [81] Y.-C. Chang et al., "Realization of mid-infrared graphene hyperbolic metamaterials," *Nature Commun.*, vol. 7, Feb. 2016, Art. no. 10568.
- [82] M. Her, R. Beams, and L. Novotny, "Graphene transfer with reduced residue," *Phys. Lett. A*, vol. 377, no. 21/22, pp. 1455–1458, Sep. 2013, doi: [10.1016/j.physleta.2013.04.015](https://doi.org/10.1016/j.physleta.2013.04.015).



**Bartosz Janaszek** received the M.Sc. and Ph.D. degrees (with Hons.) from the Warsaw University of Technology (WUT), Warsaw, Poland, in 2016 and 2022, respectively. His M.Sc. Diploma work has been selected by the Polish Committee of Optoelectronics (PKOOpto) as the best thesis in the field of optoelectronics in 2016. Since 2017, he has been a Research Associate with the Institute of Microelectronics and Optoelectronics, WUT, engaged in realization of project funded by the national and international entities. His principal research interests include metamaterials, photonic band gap materials, electromagnetic simulations, and applications of artificial intelligence. Bartosz is an author of several scientific papers, including articles in peer-reviewed journals. Since 2018, he was a Reviewer of renowned international journals, including IEEE and OSA Publishing.



**Anna Tyszk-Zawadzka** received the M.Sc. and Ph.D. degrees in quantum electronics from the Faculty of Electronics and Information Technology, Warsaw University of Technology (WUT), Poland, in 1991 and 1996, respectively. In 1996, she joined the Optoelectronics Division, Institute of Microelectronics and Optoelectronics, WUT. She is an Assistant Professor. In March 1995, she received a grant from the Foundation of Polish Science. Her principal research interests include laser physics, integrated optics and optoelectronics, photonic band gap materials, and hyperbolic metamaterials. In 1997, she was the recipient of the Prime Minister Prize for her dissertation thesis.

**Paweł Szczepański** received the M.Sc. degree in optoelectronics, the Ph.D. degree, the D.Sc. degree in laser physics, and the Professorship from the Warsaw University of Technology, Warsaw, Poland, in 1981, 1988, and 1994, respectively. In 2000, he became a Tenured Professor. He is also a Professor with the National Institute of Telecommunications, Warsaw, Poland. His principal research interests include laser physics, integrated optics and optoelectronics, passive and active photonic band gap materials, microlasers, and hyperbolic metamaterials. Prof. Szczepański is a Member of the Optical Society of America, SPIE, Polish Committee of Optoelectronics, and Section of Optoelectronics of the Committee for Electronics and Telecommunications of the Polish Academy of Sciences.